

Role of Polyradicals in Predicting Chain Length Distribution and Gelation for Radical Polymerization with Transfer to Polymer

Piet D. Iedema* and Huub C. J. Hoefsloot

Department of Chemical Engineering, University of Amsterdam, Nieuwe Achtergracht 166, 1018 WV Amsterdam, The Netherlands

Received April 14, 2004; Revised Manuscript Received September 29, 2004

ABSTRACT: A Galerkin finite element method (GF) model using pseudo-distributions was developed to predict the full two-dimensional chain length number of radical sites per chain distribution (CLD/RSD) for radical polymerization in a CSTR with transfer to polymer, without and with termination by recombination. A special variant deals with gelation using recently developed ideas involving the sol and gel moments of all chains present. The overall chain length distributions were compared to those obtained from Monte Carlo (MC) simulations, yielding almost perfect agreement in cases without and with termination by recombination, even when gelation occurs. GF models and MC simulations predict identical gel points and weight fractions gel. With increasing transfer to polymer rate coefficient k_{tp} the CLDs become broader until the gel point, while at further increase they become narrower again. It turns out that the monoradical assumption is not valid in the case of termination by disproportionation, when transfer to polymer rate to propagation rate is high and extremely long chains ($>10^8$) are formed (but no gel), even for a relatively low propagation-to-termination ratio. On the contrary, in the case of recombination-termination under circumstances leading to gelation, the assumption is valid for the sol molecules up to a ratio of 0.025 because of their relatively small size. The study reveals a deeper understanding of the polyradical issue in radical polymerization and in addition shows that two completely different computation methods—Galerkin FEM population balance equations and Monte Carlo simulations—yield perfectly matching results.

Introduction

In radical polymerization polymer chains with one or more radical sites, alternatively called macroradicals or living chains, are the heart of the polymerization process. Although living chains usually are present in negligible concentrations, models of radical polymerization based on differential equations (method of moments, Galerkin finite element (FEM)) have to take them explicitly into account for a correct description. In most models macroradicals are assumed to possess only one radical site (monoradical assumption). In principle, this is only correct for linear polymerization. In nonlinear polymerizations, e.g., those with transfer to polymer or incorporation of chains with a terminal double bond (TDB), multiradicals can easily be created. In the case of transfer to polymer this phenomenon is usually assumed to occur to dead chains only, but obviously they also take place at living chains, leading to polyradical chains. Although in general living chains are present in negligible concentrations, in this study we focus on situations where this no longer holds true for the longer chain lengths—as we noticed before.¹ Thus, it is unavoidable in view of this focus that we are confronted with gelation. This is therefore an important ingredient of our present study.

The issue of polyradicals has been addressed a few times before, in all cases for batch reactors only. The earliest modeling study fully taking polyradicals into account originates from Kuchanov and Pis'men.³ They derived analytical expressions for radical polymerization of diene leading to polymer cross-linking and a radical polymerization with transfer to polymer. Hamielec and co-workers devoted several papers^{2,4–6} to the effect of

polyradicals in radical polymerization with chain transfer to polymer and copolymerization with divinyl monomers. These studies were performed with the method of moments and led to the conclusion that the effect of polyradicals is not important for the propagation/termination coefficient ratio $k_p/k_t < 10^{-3}$. Tobita and Zhu⁶ addressed both cross-linking and radical polymerization by introducing the probability of a monomeric unit in a polymer chain of being a radical site, otherwise called radical site density. It was shown that the living chains under certain circumstances have a significant contribution to the weight fraction distribution of all chains in the reactor. Note that the radical site density in this study is independent of chain length. In the present study we also utilize a radical site density, but in our model it is explicitly taken into account in the population balance equations.

Concerning radical polymerization with transfer to polymer, in all studies mentioned gelation was observed to occur only if termination by recombination takes place. This was confirmed by Monte Carlo simulations on such systems.^{7,8} These studies were able to predict gel point conversions, sol and gel fractions, and chain length distributions in the pre- and post-gel regions. Since these MC simulations do not distinguish between living and dead chains, they do—properly, but implicitly—account for the existence of polyradicals. Structural requirements for gel formation in a CSTR were discussed leading to the conclusion that H-shaped structures are required for gel formation.⁹ Recently, a method based on moment generating functions was presented¹⁰ and applied on radical polymerization with transfer to polymer and incorporation of chains with a TDB that can predict molecular weight and other averages in the pre- and post-gel regime. The model explicitly accounts for polyradicals and the possibility that chains contain-

* Corresponding author: e-mail piet@science.uva.nl.

Table 1. Reaction Equations Radical Polymerization with Transfer to Polymer, 2D Chain Length, and Number of Radical Sites per Chain Formulation^a

initiator dissociation	$I_2 \xrightarrow{k_d} 2I$	(1.1)
initiation	$I + M \xrightarrow{k_i} R_{1,1}$	(1.2)
propagation	$R_{n,i} + M \xrightarrow{k_p} R_{n+1,i}$	(1.3)
termination by disproportionation	$R_{n,i} + R_{m,j} \xrightarrow{k_{tdij}} R_{n,i-1} + R_{m,j-1}$	(1.4)
termination by recombination	$R_{n,i} + R_{m,j} \xrightarrow{k_{trij}} R_{n+m,i+j-2}$	(1.5)
transfer to monomer	$R_{n,i} + M \xrightarrow{k_m} R_{n,i-1} + R_{1,1}$	(1.6)
transfer to solvent	$R_{n,i} + S \xrightarrow{k_{si}} R_{n,i-1} + R_{1,1}$	(1.7)
transfer to polymer	$R_{n,i} + R_{m,j} \xrightarrow{k_{tpjm}} R_{n,i-1} + R_{m,j+1}$	(1.8)

^a m, n = chain length; i, j = number of radical sites per chain.

Table 2. 2-D Population Balance Equations for Reaction System of Table 1^a

initiator dissociation	$\frac{dI_2}{dt} = -k_d I_2 + \frac{(I_2 - I_{2,f})}{\tau}$	(2.1)
initiation	$\frac{dI}{dt} = 2k_d I_2 - k_i MI - \frac{I}{\tau}; \quad \frac{dR_{1,1}}{dt} = k_i MI$	(2.2)
propagation	$\frac{dR_{n,i}}{dt} + k_p i M (R_{n-1,i} - R_{n,i}); \quad \frac{dM}{dt} = -k_p M \sum_{n=1}^{\infty} \sum_{i=0}^{\infty} i R_{n,i} + \frac{M_f - M}{\tau}$	(2.3)
termination by disproportionation	$\frac{dR_{n,i}}{dt} + k_d (\sum_{n=1}^{\infty} \sum_{i=0}^{\infty} i R_{n,i}) \{ (i+1) R_{n,i+1} - i R_{n,i} \}$	(2.4)
termination by recombination	$\frac{dR_{n,i}}{dt} + k_{tr} \{ \frac{1}{2} \sum_{m=1}^{n-1} \sum_{j=i}^{i+1} j (i-j+2) R_{m,j} R_{n-m,i-j+2} \} - (\sum_{n=1}^{\infty} \sum_{i=1}^{\infty} i R_{n,i}) i R_{n,i}$	(2.5)
transfer to monomer	$\frac{dR_{n,i}}{dt} + k_m M \{ (i+1) R_{n,i+1} - i R_{n,i} \}; \quad \frac{dR_{1,1}}{dt} + k_m (\sum_{n=1}^{\infty} \sum_{i=0}^{\infty} i R_{n,i}) M$	(2.6)
transfer to solvent	$\frac{dR_{n,i}}{dt} + k_s S \{ (i+1) R_{n,i+1} - i R_{n,i} \}; \quad \frac{dR_{1,1}}{dt} + k_m (\sum_{n=1}^{\infty} \sum_{i=0}^{\infty} i R_{n,i}) S$	(2.7)
transfer to polymer	$\frac{dR_{n,i}}{dt} + k_{tp} [(\sum_{n=1}^{\infty} \sum_{i=0}^{\infty} R_{n,i}) \{ (i+1) R_{n,i+1} - i R_{n,i} \} + (\sum_{n=1}^{\infty} \sum_{i=0}^{\infty} i R_{n,i}) n \{ R_{n,i-1} - R_{n,i} \}]$	(2.8)

^a + = duet means that the following rhs constitutes *one* contribution to the overall population balance.

ing radical sites undergo transfer to polymer but is not able to compute full chain length or number of radical sites distributions.

The present paper describes a new modeling approach to the polyradical problem, which for the first time in its history leads to a rigorous solution of the population balance equations in terms of radical site distributions. This allows us to demonstrate the effect of polyradicals on the chain length distribution for radical polymerization with transfer to polymer in a continuous reactor (continuous stirred tank reactor, CSTR) in systems capable of gelation. In addition, some new light is shed on the validity of the “monoradical assumption”. The overall distributions and the gel behavior were confirmed by an existing Monte Carlo method.^{7,8}

The new models were developed based on the Galerkin finite element method (FEM) of solving population balances as implemented in the PREDICI package.¹¹ We solve balance equations in two dimensions: chain length, n , and number of radical sites per chain, i ; stated otherwise, we solve the chain length/number of radical sites distribution (CLD/RSD). Two variants are employed being the “classes” and the “pseudo-distribution” approach, a combination that proved to be successful for the calculation of the 2-D chain length/degree of branching distribution problem of metallocene-catalyzed ethylene polymerization.¹² The classes model rigorously computes the balances for classes of chains with a specific number of radical sites. It is hence limited to problems with few (maximum around 10) radical sites per chain. According to the pseudo-distribution approach, the 2-D problem is reduced to a semi-1-D system by formulating the moments of the radical site distribu-

tion and solving these as a function of chain length. Since, as will be demonstrated, the radical site distribution at constant chain length possesses a standard statistical distribution shape (binomial distribution), the full 2-D CLD/RSD can be constructed in a straightforward manner. Thus, the pseudo-distribution Galerkin FEM approach allows us to rigorously solve the CLD/RSD for nongelling systems directly from kinetics without any additional assumptions. For gelling systems this can be realized by assuming that the long-chain limit of the radical site density calculated for the sol also holds for the gel. Note that we could deal with gelling systems in our population balance approach by a method explained before.¹ We formulate a cutoff chain length, below which the (sol fraction) balance equations are correctly solved, by accounting for the full (sol and gel) moments of the distributions involved. This allows us to determine the gelpoint as well as the gel weight fraction. The CLDs we calculate with the Galerkin FEM method are compared to those obtained from a Monte Carlo sampling method.^{7,8} We implemented this method in MATLAB and utilized the outcomes as a comparison basis for the CLDs and gel fraction as predicted by our new Galerkin FEM method for both gelling and nongelling systems.

The structure of this paper is as follows. We start with the derivation of the population balance equations for the pseudo-distribution model. They are compared to the classical equations valid under the monoradical assumption. Furthermore, the variant of the model applicable in the gel regime is explained. The main features of the Monte Carlo sampling method for this case are briefly summarized. Then, we discuss results

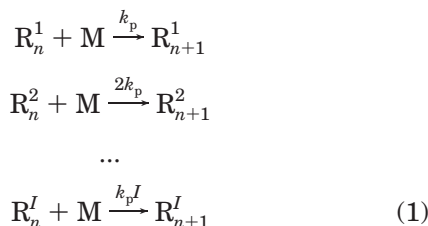
for systems with disproportionation only, without gel formation, especially showing the contribution of living, multiradical chains. Subsequently, gelling systems are addressed, and results for varying transfer to polymer rates are presented and compared to the MC results. Finally, some interesting conclusions about the methods used are drawn.

Model Formulation

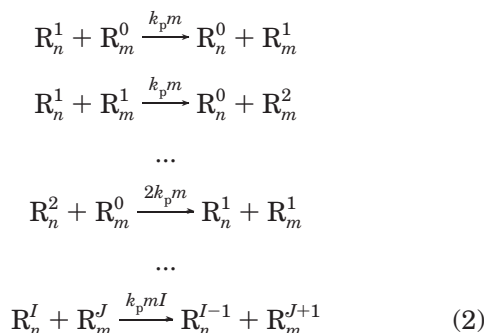
Reaction equations are listed in Table 1. The 2-D formulation of the population balance equations is given in Table 2. This system is identical to that of ref 5. Note that the second subscript of $R_{n,i}$ denotes the number of radical sites per chain; hence, chains with $i = 0$ represent what usually is called “dead” chains. The transfer to polymer reaction obviously is responsible for the creation of polyradicals, as appears from the term $R_{n,i-1}$ on the rhs in eq 2.8 (Table 2). Next we explain the two versions of the Galerkin FEM model that we have developed: the classes and the pseudo-distribution model.

Classes Model. Separate distributions R_n^I are defined for each class of chains with a specific number of radical sites, I . Note that the classical problem (monoradical assumption) is usually formulated with two classes: class zero or dead chains and class one or living chains. Formulating this model anticipates the expectation that transition regimes exist, where the monoradical assumption no longer holds, while the number of radical sites per chain is still low.

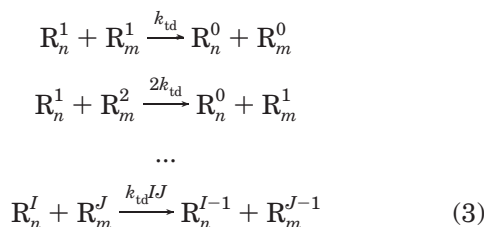
propagation reactions:



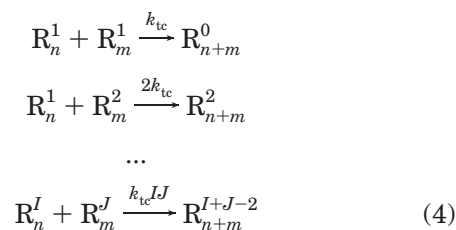
transfer to polymer reactions:



disproportionation termination:



recombination termination:



We employ classes models with up to 11 classes. Note that the implementation of the termination reactions in a model with I classes requires the implementation of I^2 pairs of reaction equations. Thus, we see that many more classes rapidly lead to a huge implementation task, and the classes method is not appropriate for problems with many radical sites per chain.

We now first present and discuss some results from classes model calculations for nongelling systems with limited numbers of radical sites per chain to explore various distribution shapes. CLDs per number of RS class are shown in Figure 1 for kinetic coefficient values given in the caption. From the calculated $R_{n,i}$ the average number of radical sites per chain $\bar{N}_{RS}(n)$, the earlier discussed⁶ radical site density ρ_{RS} , and the radical site distribution polydispersity $D_{RS}(n)$ all as a function of chain length can be calculated:

$$\begin{aligned} \bar{N}_{RS}(n) &= \frac{\sum_{i=0}^{i_{\max}} i R_{n,i}}{\sum_{i=0}^{i_{\max}} R_{n,i}}; \quad \rho_{RS}(n) = \frac{\sum_{i=0}^{i_{\max}} i R_{n,i}}{n \sum_{i=0}^{i_{\max}} R_{n,i}} \\ D_{RS}(n) &= \frac{\sum_{i=0}^{i_{\max}} i^2 R_{n,i}}{n \sum_{i=0}^{i_{\max}} i R_{n,i}} \bigg/ \frac{\sum_{i=0}^{i_{\max}} i R_{n,i}}{n \sum_{i=0}^{i_{\max}} R_{n,i}} \end{aligned} \quad (5)$$

In the example presented $\bar{N}_{RS}(n)$ amounts to 5.58 radical sites for chains with length $n = 10^8$. Figure 2 shows the RS density and polydispersity. Note—confirming and quantifying what already was noticed in previous work⁶—that the RS density at lower chain length range decreases with n , while becoming constant at high lengths; this limiting value we will call $\rho_{RS}(\infty)$. As regards polydispersity, we compared the Galerkin FEM outcome to that inferred from the RS density and the chain length assuming a binomial distribution:

$$D_{RS}(n)_{\text{binomial}} = (1 + \rho_{RS} n - \rho_{RS}) / (\rho_{RS} n) \quad (6)$$

Almost perfect agreement is found, which leads us to the conclusion that the number distribution of radical sites at fixed chain length is well represented by a binomial distribution. This is a result that will prove to be convenient later.

Pseudo-Distribution Model. Tables 3 and 4 contain the equations for the zeroth and first number of radical sites per chain (RS) moments, R_n and Φ_n^1 , respectively. They have been derived from the full 2-D equations in Table 2 by multiplying with the number of radical sites

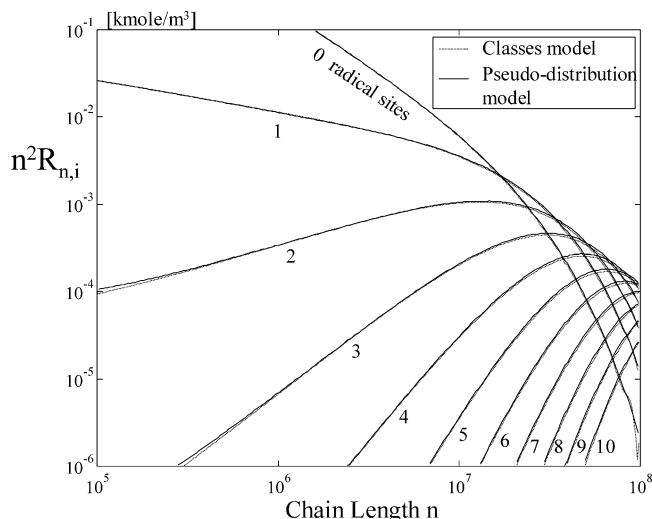


Figure 1. Length distributions for chains with 0–10 radical sites from Galerkin FEM 11 classes and pseudo-distribution models. Kinetic data: feed monomer concentration: $M_f = 16.75$ kmol/m³; average residence time CSTR $\tau = 30$ s; $k_p = 5 \times 10^4$ m³/(kmol s); $k_{tc} = k_{td} = 10^6$ m³/(kmol s); $k_{tp} = 0.15$ m³/(kmol s); conversion $x = 0.855$.

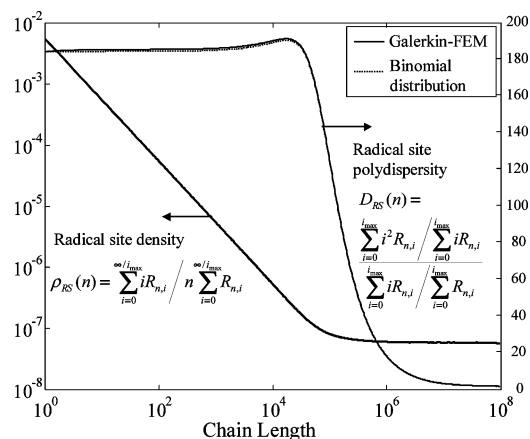


Figure 2. Radical site density $\rho_{RS}(n)$ and polydispersity $D_{RS}(n)$ vs chain length. Perfect agreement $\rho_{RS}(n)$ from pseudo-distribution model with $\rho_{RS}(n)$ from classes model. D_{RS} from Galerkin FEM classes model practically coinciding with D_{RS} from binomial distribution (eq 6). Kinetic data of Figure 1.

per chain i and subsequent summation over i . The RS moments are defined as

$$R_n = \sum_{i=1}^{\infty} R_{n,i}; \quad \Phi_n^1 = \sum_{i=1}^{\infty} i R_{n,i}; \quad \Phi_n^2 = \sum_{i=1}^{\infty} i^2 R_{n,i} \quad (7)$$

Note that physically R_n and Φ_n^1 represent the total concentration of polymer chains of length n and the total concentration of radical sites on chains with length n , respectively. The radical site density earlier introduced⁶ is now defined in terms of distributions:

$$\rho_{RS}(n) = \Phi_n^1 / (R_n n) \quad (8)$$

Total moments required in the model are

$$\lambda_{10} = \sum_{n=1}^{\infty} n \sum_{i=1}^{\infty} R_{n,i}; \quad \lambda_{01} = \sum_{n=1}^{\infty} \sum_{i=1}^{\infty} i R_{n,i} \quad (9)$$

These moments physically represent the molar concen-

tration of monomers incorporated in polymer chains and the total molar concentration of radical sites present, respectively. Derivation of the equations in Tables 3 and 4 proceeds in a straightforward way for most mechanisms, but the production terms of the recombination contribution deserves some closer attention. The original 2-D formulation of this contribution reads

$$\frac{dR_{n,i}}{dt} + = \frac{1}{2} k_{tc} \sum_{m=1}^{n-1} \sum_{j=1}^{i+1} j(i-j+2) R_{m,j} R_{n-m,i-j+2} \quad (10)$$

The zeroth RS moment distribution R_n can be derived by taking the following steps:

$$\begin{aligned} \frac{dR_n}{dt} + &= \frac{1}{2} \sum_{m=1}^{n-1} \sum_{i=0}^{\infty} \sum_{j=1}^{i+1} j(i-j+2) R_{m,j} R_{n-m,i-j+2} \\ &= \frac{1}{2} k_{tc} \sum_{m=1}^{n-1} \left\{ R_{m,1} \sum_{i=0}^{\infty} i R_{n-m,i} + 2 R_{m,2} \sum_{i=0}^{\infty} i R_{n-m,i} + \right. \\ &\quad \left. 3 R_{m,1} \sum_{i=0}^{\infty} i R_{n-m,i} + \dots \right\} \\ &= \frac{1}{2} k_{tc} \sum_{m=1}^{n-1} \sum_{j=0}^{\infty} j R_{m,j} \sum_{i=0}^{\infty} i R_{n-m,i} \\ &= \frac{1}{2} k_{tc} \sum_{m=1}^{n-1} \Phi_m^1 \Phi_{n-m}^1 \end{aligned} \quad (11)$$

Likewise, the first RS moment follows by

$$\begin{aligned} \frac{d\Phi_n^1}{dt} + &= \frac{1}{2} k_{tc} \sum_{m=1}^{n-1} \sum_{i=0}^{\infty} \sum_{j=1}^{i+1} i j (i-j+2) R_{m,j} R_{n-m,i-j+2} \\ &= \frac{1}{2} k_{tc} \sum_{m=1}^{n-1} \left\{ R_{m,1} \sum_{i=0}^{\infty} (i-1) i^2 R_{n-m,i} + \right. \\ &\quad \left. 2 R_{m,2} \sum_{i=0}^{\infty} i^3 R_{n-m,i} + \right. \\ &\quad \left. 3 R_{m,1} \sum_{i=0}^{\infty} (i+1) i^2 R_{n-m,i} + \dots \right\} \\ &= \frac{1}{2} k_{tc} \sum_{m=1}^{n-1} \sum_{j=0}^{\infty} j R_{m,j} \sum_{i=0}^{\infty} i (i+j-2) R_{n-m,i} \\ &= k_{tc} \sum_{m=1}^{n-1} \left\{ \Phi_m^1 \Phi_{n-m}^2 - \Phi_m^1 \Phi_{n-m}^1 \right\} \end{aligned} \quad (12)$$

It can be noticed in Table 3 that the propagation terms of the total polymer concentration R_n are expressed in the higher RS moment Φ_n^1 . Furthermore, it turns out that disproportionation and transfer to polymer do not affect the total polymer distribution R_n , whereas they do have a contribution on the level of Φ_n^1 .

It can now be observed that the pseudo-distribution model of Tables 3 and 4 transforms into the classical model based on the monoradical assumption when the consequences of this assumption on the equations of the new model are considered. If this assumption holds true, then the first RS moment distribution Φ_n^1 becomes equal to the usual concentration of living chains $R_{n,1}$, while the second (and higher) RS moments become

Table 3. Zeroth Number of Radical Sites (RS) Moment Population Balance Equations for Reaction System of Table 1

initiation	$\frac{dR_1}{dt} = k_i MI$	(3.1)
propagation	$\frac{dR_n}{dt} = k_p M(\Phi_{n-1}^1 - \Phi_n^1); \quad \frac{dM}{dt} = -k_p M \lambda_{01} + \frac{M_f - M}{\tau}$	(3.2)
termination by disproportionation	$\frac{dR_n}{dt} = 0$	(3.3)
termination by recombination	$\frac{dR_n}{dt} = k_{tc} [\frac{1}{2} \sum_{m=1}^{n-1} \Phi_m^1 \Phi_{n-m}^1 - \lambda_{01} \Phi_n^1]$	(3.4)
transfer to monomer	$\frac{dR_{n,i}}{dt} = 0; \quad \frac{dR_1}{dt} = k_m \lambda_{01} M$	(3.5)
transfer to solvent	$\frac{dR_n}{dt} = 0; \quad \frac{dR_1}{dt} = k_m \lambda_{01} S$	(3.6)
transfer to polymer	$\frac{dR_n}{dt} = 0$	(3.7)

Table 4. First Number of Radical Sites (RS) Moment Population Balance Equations for Reaction System of Table 1

propagation	$\frac{d\Phi_n^1}{dt} = k_p(\Phi_{n-1}^2 - \Phi_n^2)$	(4.1)
termination by disproportionation	$\frac{d\Phi_n^1}{dt} = -k_{td} \lambda_{01} \Phi_n^1$	(4.2)
termination by recombination	$\frac{d\Phi_m^1}{dt} = k_{tc} [\sum_{m=1}^{n-1} (\Phi_m^1 \Phi_{n-m}^1 - \Phi_m^1 \Phi_{n-m}^1) - \lambda_{01} \Phi_n^2]$	(4.3)
transfer to monomer	$\frac{d\Phi_n^1}{dt} = -k_m M \Phi_n^1$	(4.4)
transfer to solvent	$\frac{d\Phi_n^1}{dt} = -k_s S \Phi_n^1$	(4.5)
transfer to polymer	$\frac{d\Phi_n^1}{dt} = k_{tp} \{-\lambda_{10} \Phi_n^1 + \lambda_{01} n R_n\}$	(4.6)

equal to $\Phi_n^1 = R_{n,1}$. This implies that all the equations of Table 4 directly should apply to the classical living chain population balance equations, which easily can be confirmed. The equations of Table 3 still apply to the *sum* of living and dead chains. We see that the classical dead equations are exactly reproduced when subtracting equations of Table 4 from those in Table 3. Thus, we see that under the limiting case of the monoradical assumption our new model properly transforms into the classical one.

The new model as described by Tables 3 and 4 shows that a *closure* problem exists due to the contributions of the propagation and recombination steps: solving the lower moments R_n and Φ_n^1 requires knowing the higher moments Φ_n^1 and Φ_n^2 , respectively. Obviously, the possibilities of a closure relationship depend on the shape of the RS distribution at given chain length, which from the classes model was found to obey a binomial distribution. This implies that Φ_n^2 can be expressed in lower moments in the following *exact* manner (similar to eq 6):

$$\Phi_n^2 = (1 + \rho_{RS} n - \rho_{RS}) \rho_{RS} n \quad (13)$$

where ρ_{RS} is given by eq 8. Thus, we see that the pseudo-distribution model can be rigorously solved without making any additional assumption. Obviously, one would then expect this solution to coincide with that from the classes model for lower numbers of radical sites per chain. This is indeed what we find—apart from small numerical errors—as demonstrated by Figure 1. In addition, perfect agreement turns out to exist regarding the RS density ρ_{RS} as calculated from both models (Figure 2).

Systems with Gelation. In the PREDICI implementation of the Galerkin FEM models discussed so far gelation leads to a mismatch in the mass balance. This mismatch is detected by comparing the total amount of

monomer units represented by the calculated distribution λ_{10} to the monomer units converted xM_f (x is conversion and M_f is monomer feed concentration). When

$$\lambda_{10} = \sum_{n=1}^{\infty} n R_n < x M_f \quad (14)$$

gelation occurs. The solutions containing such a mismatch are obviously not correct. However, the derived models can still be applied on gelling systems after a modification according to a method we have developed before in the context of a monoradical model.¹ We define a “cutoff” length n_c leading to a split-up into sol and gel terms of the total moments λ_{10} and λ_{01} as featured in the pseudo-distribution model equations:

$$\lambda_{10} = \lambda_{10}^{\text{sol}} + \lambda_{10}^{\text{gel}} = \sum_{n=1}^{n_c} n R_n + \sum_{n=n_c+1}^{\infty} n R_n \quad (15)$$

$$\lambda_{01} = \lambda_{01}^{\text{sol}} + \lambda_{01}^{\text{gel}} = \sum_{n=1}^{n_c} \Phi_n^1 + \sum_{n=n_c+1}^{\infty} \Phi_n^1 \quad (16)$$

We now assume that in gelling systems the gel part of the distributions cannot be described by the model as the chain length of this part goes to infinity; this is the part “beyond” the cutoff length n_c . Still, the part below n_c , the “sol” distributions can be described, and they should obey the population balance equations of Tables 3 and 4. This is only correct when the *total* moments λ_{10} and λ_{01} are inserted in these equations, rather than the sol parts of the moments corresponding to the sol distributions, $\lambda_{10}^{\text{sol}}$ and $\lambda_{01}^{\text{sol}}$. Solving the gel variant of the model therefore requires a different solution strategy. For nongelling systems both conversion and total moments follow as parts of the results, but under gelation

we want to impose the moments as inputs at *given conversion*. This is feasible since in our model we assume that gelation does not affect conversion (e.g., no gel effect on termination). Now, both moments are directly coupled to conversion, λ_{10} representing monomers converted and λ_{01} being related to monomer consumption by eq 3.2 in Table 3, so we can easily compute λ_{10} and λ_{01} from conversion. At this stage the equation system under gelling conditions has one extra degree of freedom. For instance, if $\lambda_{01}^{\text{sol}}$ as defined by eq 16 is taken as such, one may vary it, yielding varying results for $\lambda_{10}^{\text{sol}}$. Now, it should be realized that in reality it is not very probable that this degree of freedom exists in view of the constant RS density at long chain lengths, $\rho_{\text{RS}}(\infty)$. The constant RS density implies the equality

$$\Phi_n^1 = \rho_{\text{RS}}(\infty) R_n n \quad (17)$$

which with eqs 15 and 16 leads to a fixed ratio between $\lambda_{01}^{\text{gel}}$ and $\lambda_{10}^{\text{gel}}$:

$$\lambda_{01}^{\text{gel}}/\lambda_{10}^{\text{gel}} = \rho_{\text{RS}}(\infty) \quad (18)$$

In other words, if we assume that the gel fraction possesses the same RS density as the long chain limit of the sol fraction, $\rho_{\text{RS}}(\infty)$, the gel variant of the pseudo-distribution model has only one solution. Under this assumption it is then in principle able to *predict* the gel fraction as well as the CLD of the sol fraction. It is obvious that calculations with the model should demonstrate how well the sol CLD is described and whether any dependency exists of the results on the choice of the cutoff limit n_c .

Similarly, a gel variant of a two-classes model (monoradical assumption) has been developed in the same manner as before.¹ The assumption of eq 18 here boils down to supposing the concentration the ratio between living and dead chains in the gel fraction to be equal to that at the longest chain lengths calculated.

Monte Carlo Simulations. The Monte Carlo simulation technique we apply here on radical polymerization with transfer to polymer and recombination termination has first been described by Tobita.^{7,8} In this section the main aspects are summarized. The MC method considers a branched molecule to be composed of primary polymers (pp's), linear chains of which growth has started from monoradicals or from secondary radical sites at other pp's, created by transfer to polymer, and stopped by a certain termination mechanism. Pp's can possess one or more branch points, at which other pp's have been growing. Instantaneous growth of primary polymers is assumed leading to a Flory length distribution. For each pp a residence time t and a length n must be determined. t is sampled from the residence time distribution (RTD) in a CSTR:

$$F(\theta) = \exp(-\theta) \quad (19)$$

where the reduced residence time $\theta = t/\tau$, τ being the average residence time. The length of the first linear element is sampled on a *weight* basis (in fact, a *monomer unit* on the first element is sampled) from

$$w_n = \frac{n}{\bar{n}^2} \exp\left(-\frac{n}{\bar{n}}\right) \quad (20)$$

the average chain length \bar{n} being given by

$$\bar{n} = k_p M / \{(k_{\text{td}} + k_{\text{tc}})\lambda_{01} + k_{\text{tp}}\lambda_{10}\} \quad (21)$$

Next, a check is made whether this element is connected to a second one, grown at the same instant, by a recombination reaction. This is realized by sampling a random number between 0 and 1 (rand(1)) and assuming the presence of connection when rand(1) < P_{tc} , where

$$P_{\text{tc}} = k_{\text{tc}}\lambda_{01}/(k_{\text{tc}}\lambda_{01} + k_{\text{td}}\lambda_{01}k_{\text{tp}}\lambda_{10}) \quad (22)$$

If connection is at hand, the length of the connected element is sampled from a *number* distribution, since connection can only happen at one terminal end:

$$n_n = \frac{1}{\bar{n}} \exp\left(-\frac{n}{\bar{n}}\right) \quad (23)$$

The length of the first pp (0th generation) ultimately becomes the sum of lengths of the two connected elements. Next, the number of branch points on the first pp is determined. The longer a pp stays in the reactor, the higher its probability of receiving branch points, or branching density on a pp is proportional to residence time θ :

$$\rho(\theta) = \bar{\rho}\theta \quad (24)$$

The average branching density $\bar{\rho}$ is related to the transfer to polymer rate:

$$\bar{\rho} = k_{\text{tp}}\lambda_{01}\tau \quad (25)$$

The actual number of branch points, m , on the first pp follows from a binomial distribution, given $\rho(\theta)$ and n :

$$p(m) = \binom{n}{m} \rho^m \rho^{(n-m)} \quad (26)$$

The residence time u of each of these pp's having grown on the first pp should be *smaller* than θ , or $0 < u < \theta$. They are sampled from the conditional (given the connection to the pp created at θ) probability:

$$CP_a(u|\theta) = u/\theta \quad (27)$$

because of the linear dependence on exposure time, the branching density being constant. Lengths of these pp's are sampled from the number fraction distribution, n_n , eq 23 (connection on terminal end only). Again, these pp's could have been created by recombination, in which case they are connected to a second linear element. The check proceeds as before.

Now, the probability that the first pp has itself been initiated at a secondary radical site on a pp previously created must also be considered. This is checked by sampling a random number between 0 and 1 and accepting connection when rand(1) < P_b , where the branching probability is given by

$$P_b = k_{\text{tp}}\lambda_{10}/\{(k_{\text{tp}} + k_{\text{td}})\lambda_{01} + k_{\text{tp}}\lambda_{10}\} \quad (28)$$

If connection is at hand, the length of the previous pp is determined by sampling from the *weight* fraction distribution, eq 20, since the connection may be located at any monomer unit on it. Then, again a check is made of it being connected to a second linear element by

recombination. The residence time z is determined by realizing that previous with respect to θ means a longer residence time than θ : $\theta < z < \infty$. Thus, sampling takes place from a conditional probability expression containing the RTD (eq 19):

$$CP_i(z|\theta) = \frac{1 - F(z)}{1 - F(\theta)} \quad (29)$$

Finally, the number of branch points on this previous pp is determined, using eqs 24–26, but now with residence time z . Lengths and residence times of pp's connected to these branch points are sampled as before. The whole procedure is then repeated for the pp's of generation 1—all pp's connected to the branch points on the (one or two) pp's of generation 0—and subsequent generations.

The MC algorithm produces a range of polymer molecules with specified lengths and numbers of branch points. Since sampling essentially is performed on a *weight* basis, counting numbers of molecules in chain length intervals yields the *weight fraction distribution*. This has interesting consequences for systems with possibility of gelation. A “gel molecule” is encountered in the algorithm, when the growth process does not stop, typically generating increasing numbers of branch points at each next generation. This is detected by checking whether the number of generation exceeds a certain limit. If so, the growth process is stopped. Obviously, then the size of this molecule is yet undefined. However, the number of such “unknown” molecules as relative to the total number of molecules in fact represents their weight fraction. In other words, the weight fraction of the gel is computable in this system. This allows comparison to gel fractions and sol weight fraction distributions obtained with the Galerkin FEM methods.

Results

Termination by Disproportionation Only: No Gelation. Calculations were carried out with the Galerkin FEM pseudo-distribution model and the Monte Carlo algorithm for kinetic conditions as mentioned in the caption of Figure 3. As appears from this figure under these conditions the CLDS is extremely broad. For purely computational reasons the maximum chain length in the Galerkin FEM calculations is set at 10^{10} , which turns out to lead to a negligible error in the mass balance, and in the Monte Carlo simulations to 10^8 . Although the distributions possess tails even beyond these limits, the weight fraction of these tails is negligible. By performing the gelation check of eq 14, it was ensured that no gelation takes place, which is in line with previous observations.^{1,6,9} In the Monte Carlo simulations it was also seen that chains $> 10^8$ ultimately would lead to molecules of finite length, although this took excessive computation time. Figure 3 shows that the overall CLDs of the Galerkin FEM model and the Monte Carlo simulations are in complete agreement. From the separate CLDs for chains with 0, 1, 2, etc., radical sites the remarkable contribution of chains with greater numbers of radical sites becomes immediately clear. Note, from Figure 4, that the average number of radical sites at $n = 10^{10}$ amounts to 5000. In view of the narrow RS distribution (binomial) at fixed chain length, we infer that the CLD tail at n is around 10^{10} consists of chains with thousands of radical sites. Figure

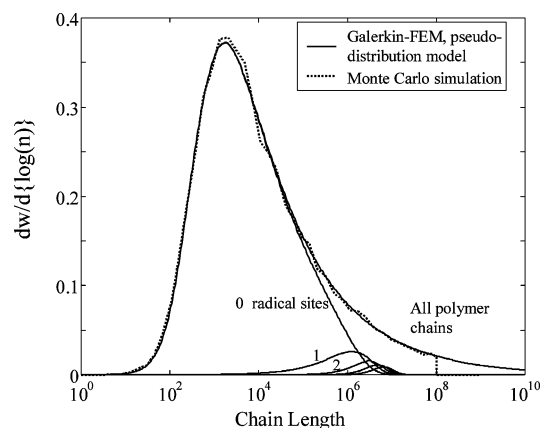


Figure 3. Length distributions for chains with 0–5 radical sites from Galerkin FEM pseudo-distribution models and overall CLDs from pseudo-distribution model and Monte Carlo simulation (40 000 molecules). Kinetic data: $k_p = 5 \times 10^3 \text{ m}^3/(\text{kmol s})$; $k_{tc} = k_{td} = 5 \times 10^6 \text{ m}^3/(\text{kmol s})$; $k_{tp} = 25 \text{ m}^3/(\text{kmol s})$; conversion $x = 0.456$; $\lambda_{01} = 5.58 \times 10^{-6} \text{ kmol/m}^3$; $\lambda_{10} = 7.65 \text{ kmol/m}^3$; $P_b = 0.7706$; $\bar{\rho} = 4.19 \times 10^{-3}$; $\bar{n} = 190$ (eq 21). MC simulations stopped when $n > 10^7$ predominately living chains with many radical sites (up to 5000, see Figure 4).

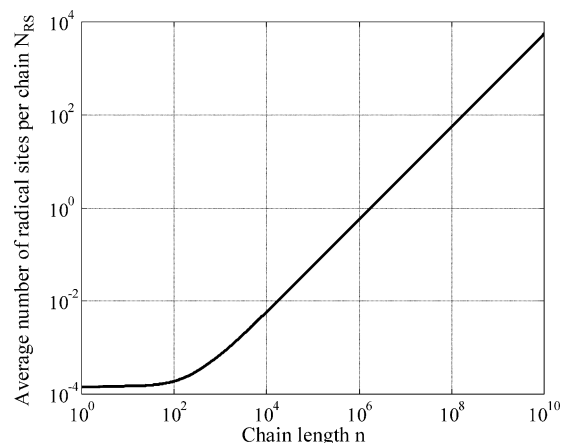


Figure 4. Average number of radical sites per chain as a function of chain length. Kinetic data of Figure 3.

5 finally makes clear that the correct overall CLD cannot be predicted under the monoradical assumption, since then a much narrower CLD is computed. In other words, we conclude that the perfect agreement between the Galerkin FEM model and Monte Carlo simulations could only be achieved, when properly accounting for polyradicals in the former.

Termination by Disproportionation and Recombination: Gelation. Calculations have been performed for cases with equal termination by recombination and disproportionation rate coefficients. Further kinetic data are given in the caption to Figure 6. Under these circumstances we will again check the validity of the monoradical assumption. We choose the propagation-to-termination ratio $k_p/(k_{tc} + k_{td})$ to equal 0.025. This is a factor of 25 larger than the critical value of 0.001, above which the monoradical assumption earlier² was found to fail for a similar radical polymerization in a batch reactor (using a different method: the method of moments). The transfer to polymer rate has been varied, and we observed that the Galerkin FEM model and the Monte Carlo simulations yield exactly the same gel point: at $k_{tp} = 0.14 \text{ m}^3/(\text{kmol s})$. For higher k_{tp} values the gel variants of the Galerkin FEM pseudo-distribu-

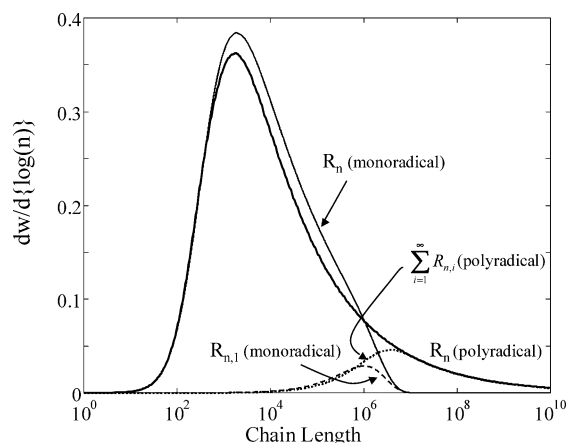


Figure 5. Chain length distributions from Galerkin FEM 2-classes (classical living and dead chain, monoradical assumption) and pseudo-distribution model (polyradical); overall polymer chain distributions R_n and contribution of living (one or more radical sites) chain distributions. Kinetic data of Figure 3. Accounting for polyradicals yields significantly broader CLD and more important contribution of living chains.

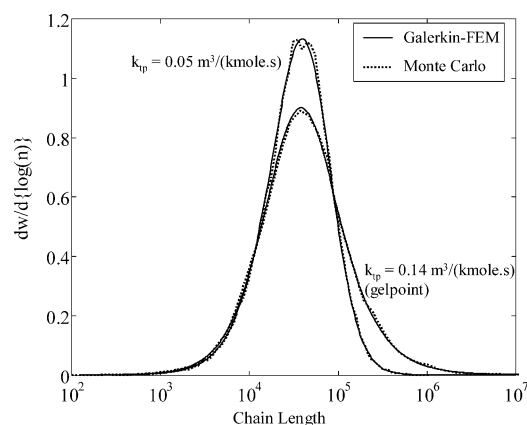


Figure 6. Length distributions (in the presence of termination by recombination) from Galerkin FEM pseudo-distribution model and Monte Carlo simulation (40 000 molecules) for two values of k_{tp} ; below and at gel point. Kinetic data: $k_p = 5 \times 10^4 \text{ m}^3/(\text{kmol s})$; $k_{tc} = k_{td} = 10^6 \text{ m}^3/(\text{kmol s})$; conversion $x = 0.856$; $\lambda_{01} = 3.945 \times 10^{-6} \text{ kmol/m}^3$; $\lambda_{10} = 14.33 \text{ kmol/m}^3$; $P_c = 0.45838$ ($k_{tp} = 0.05 \text{ m}^3/(\text{kmol s})$)/0.3987 ($k_{tp} = 0.14 \text{ m}^3/(\text{kmol s})$); $P_b = 0.08324$ (0.05)/0.2027 (0.14); $\bar{\rho} = 5.92 \times 10^{-6}$ (0.05)/ 1.66×10^{-5} (0.14); $\bar{n} = 14\,077$ (0.05)/12243 (0.14) (eq 21).

tion and two-classes (monoradical assumption) model have been used. From Figure 6 (below and at gel point) and Figure 7 (above gel point) we see that CLDs calculated from Galerkin FEM models and Monte Carlo simulations are in almost perfect agreement. Monte Carlo samples are typically 40 000 molecules (sol part in case of gelation); taking larger samples yields even smoother curves and better agreement. Figures 6 and 7 show that the CLD becomes broader with increasing k_{tp} until the gel point. Beyond the gel point they become narrower again, a phenomenon already observed from Monte Carlo simulations of a batch reactor system before.¹³ We conclude that both the Galerkin FEM models (gel variants) and the Monte Carlo simulations fulfill the requirement that the CLDs (and gel fraction) calculated are independent of cutoff length as long as it is chosen above the longest molecule of the sol fraction. Furthermore, we see that the equal radical site density assumption of the Galerkin FEM models (eq 18) proves to be in agreement with the outcomes of the Monte Carlo simulations. Figure 7 shows that the

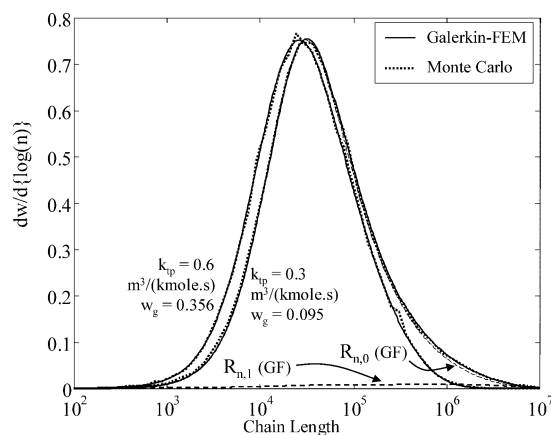


Figure 7. Length distributions (presence of termination by recombination) from Galerkin FEM pseudo-distribution model and Monte Carlo simulation (80 000 molecules, including gel molecules) for two values of k_{tp} ; above gel point: $w_g = 0.095$ ($k_{tp} = 0.3 \text{ m}^3/(\text{kmol s})$)/0.356 ($k_{tp} = 0.6 \text{ m}^3/(\text{kmol s})$); CLDs represent sol fraction only. Kinetic data as in Figure 6. $P_c = 0.32368$ ($k_{tp} = 0.3 \text{ m}^3/(\text{kmol s})$)/0.2393 ($k_{tp} = 0.6 \text{ m}^3/(\text{kmol s})$); $P_b = 0.35265$ (0.3)/0.5214 (0.6); $\bar{\rho} = 3.55 \times 10^{-5}$ (0.3)/ 7.1×10^{-5} (0.6); $\bar{n} = 9940$ (0.3)/7349 (0.6) (eq 21). Major part of chains possess 0 radical sites ($R_{n,0}$, calculated with the Galerkin FEM model), minor contribution of chains with radicals (see $R_{n,1}$ at the bottom of the figure).

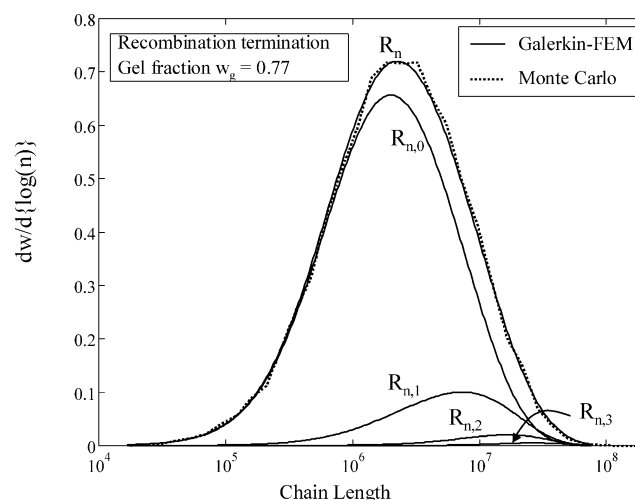


Figure 8. Sol fraction length distributions (presence of termination by recombination) from Galerkin FEM pseudo-distribution model and Monte Carlo simulation (100 000 molecules, including gel molecules) for extremely high propagation-to-termination ratio: $k_p/(k_{tc} + k_{td}) = 1$; above gel point: $w_g = 0.77$. Kinetic data: $k_p = 5 \times 10^5 \text{ m}^3/(\text{kmol s})$; $k_{tc} = k_{td} = 2.5 \times 10^5 \text{ m}^3/(\text{kmol s})$; $k_{tp} = 0.1 \text{ m}^3/(\text{kmol s})$; conversion $x = 0.897$; $\lambda_{01} = 5.8 \times 10^{-7} \text{ kmol/m}^3$; $\lambda_{10} = 15.02 \text{ kmol/m}^3$; $P_c = 0.0809$; $P_b = 0.8382$; $\bar{\rho} = 1.74 \times 10^{-6}$; $\bar{n} = 4.818 \times 10^5$ (eq 21). Contribution of chains with radical sites significant here ($R_{n,1}$ through $R_{n,3}$ shown).

chains possessing radical sites are present in only minor concentrations in comparison to dead chains. This agrees with the fact that the two-classes model (monoradical assumption) yields practically identical results as the pseudo-distribution model. In other words, even for this high propagation-to-termination ratio the monoradical assumption still yields good results.

To further explore the validity of the monoradical assumption, we performed simulations at the extremely high propagation-to-termination ratio of one. The resulting CLDs are presented in Figures 8 and 9. Here, the contribution of chains with radicals sites is signifi-

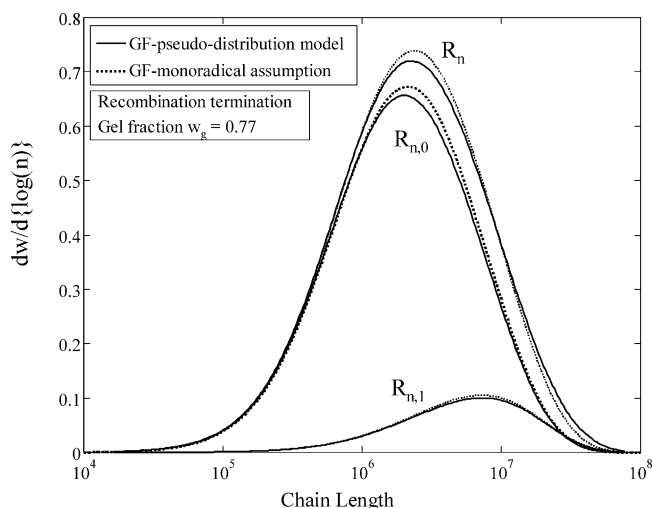


Figure 9. Length distributions (presence of termination by recombination) from Galerkin FEM pseudo-distribution and 2-classes (monoradical assumption) model for extremely high propagation-to-termination ratio: $k_p/(k_{tc} + k_{td}) = 1$; above gel point: $w_g = 0.77$. Kinetic data as in Figure 8. Impact of monoradical assumption is visible, but small.

cant, and the Galerkin FEM model under the monoradical assumption yields CLDs that are visibly deviating, but still to a low extent. We conclude that in the presence of termination by recombination deviations from the monoradical assumption are much smaller than without recombination. It should be noticed, however, that calculations with the case of disproportionation only were performed with a much higher ratio of transfer to polymer to propagation. Increasing k_{tp} for the case with recombination would lead to stronger deviations from the monoradical case as well, but this is severely limited by gelation: a further increase would rapidly lead to 100% gelation. The value of k_{tp}/k_p has a strong impact on the presence of chains with many radical sites. A high value (disproportionation only) leads to significant concentrations of chains with many radical sites (several thousands, see Figure 4), whereas for a low value the number of radical sites per chain is limited to less than 10. Stated differently, with only disproportionation extremely large molecules can exist that still are not gel molecules (infinitely large) but carry many radical sites. With recombination, gelation can occur, leading to relatively small sol molecules with mainly 0 or 1 radical site. Obviously, in the latter case the gel fraction possesses many radical sites.

Figure 10 shows the radical site density ρ_{RS} vs chain length for various transfer to polymer rates. They follow the same trend as the curve for the case with disproportionation only (Figure 2). Figure 11 finally plots the weight fraction gel w_g vs the transfer to polymer rate as calculated by the Galerkin FEM model and by Monte Carlo simulations. They exactly coincide.

Conclusions

We developed a Galerkin FEM model based on pseudo-distributions that is able to predict the full two-dimensional chain length number of radical sites per chain distribution for radical polymerization in a CSTR with transfer to polymer, without and with termination by recombination. A classes model proved—for a limited number of radical sites per chain—that the number of radical sites per chain obeys a binomial distribution at fixed chain length. This solves the closure problem of

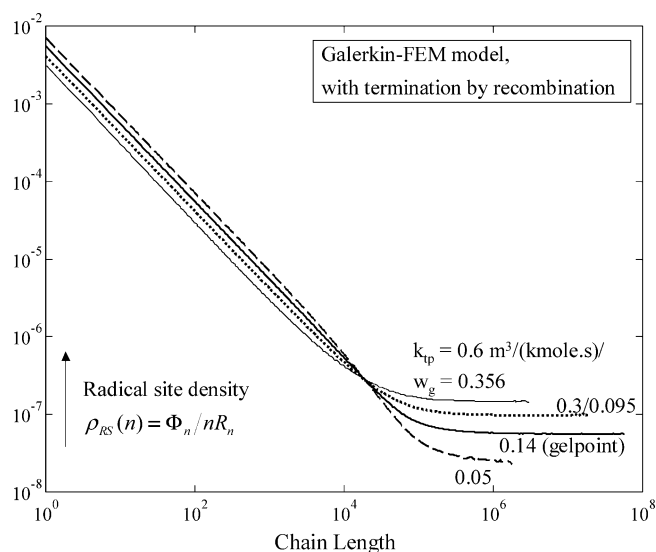


Figure 10. Radical site density vs chain length for various transfer to polymer rates in the presence of termination by recombination. Kinetic data as in Figures 6 and 7. ρ_{RS} decreasing at lower chain length, reaching plateau at higher lengths. RSDs represent sol fraction only.

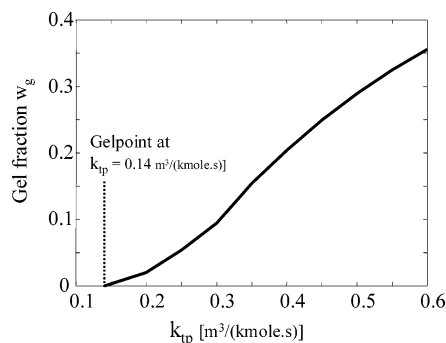


Figure 11. Gel fraction w_g vs transfer to polymer rate coefficient (in the presence of termination by recombination) according to Galerkin FEM pseudo-distribution model and Monte Carlo simulations (coinciding). Kinetic data as in Figure 6.

the pseudo-distribution model and simplifies it to a great extent. Special variants of the GF models were constructed dealing with gelation based on earlier developed ideas and involving the complete (sol and gel) moments of all chains present.

The overall chain length distributions calculated with the GF models were compared to those obtained from Monte Carlo simulations, yielding almost perfect agreement in cases without and with termination by recombination, even when gelation occurs. GF models and MC simulations predict identical gel points and weight fractions gel, the latter for various transfer to polymer rate coefficients. The agreement in CLD and gel predictions confirms the validity of the assumptions concerning the binomial distribution shape for chains with up to thousands of radical sites. Indirectly, from the results with gelation also confirmation was found from the MC simulations for the assumption, in the GF models, of equal radical site density of the gel to that of the longest sol chains (eq 18). CLD, gel point, and gel fraction predictions from both GF models and MC simulations turned out to be independent from the cutoff chain length as long as it is chosen larger than the longest sol chain. With increasing k_{tp} the CLDs become broader

until the gel point, while at further increase they become narrower again, as was observed before for a batch reactor.¹³

In the case of termination by disproportionation only the monoradical assumption turns out to be not valid, when transfer to polymer rate to propagation rate is high ($k_{tp}/k_p = 0.005$), leading to extremely long chains ($>10^8$), even at low $k_p/(k_{tc} + k_{td})$ (0.001). When termination by recombination occurs, we found that the assumption can be valid up to $k_p/(k_{tc} + k_{td}) = 0.025$. Note, for reference, that in earlier work² for a batch reactor the monoradical assumption was observed to hold, using the method of moments, if the ratio of propagation to termination is lower than 0.001. From our work, only in the extreme situation of $k_p/(k_{tc} + k_{td}) = 1$ a small deviation from the monoradical assumption is found. This is due to the fact that without recombination much higher k_{tp}/k_p can be chosen than when this mechanism is present. In the latter case a limit to k_{tp} exists—the 100% gelation case—that is not present in the former. In summary, with only disproportionation extremely large molecules can exist that still are not gel molecules (infinitely large) but carry many radical sites. With recombination, gelation can occur, leading to relatively small sol molecules with mainly 0 or 1 radical site. Obviously, in the latter case the gel fraction possesses many radical sites.

In conclusion, our study reveals deeper understanding of the old polyradical issue in radical polymerization. In addition, it shows two completely different computation methods—Galerkin FEM population balance equations and Monte Carlo simulations—to yield perfectly matching results.

References and Notes

- (1) Iedema, P. D.; Hoefsloot, H. C. J. *Macromol. Theory Simul.* **2002**, *11*, 410.
- (2) Zhu, S.; Hamielec, A. E. *Macromolecules* **1993**, *26*, 3131.
- (3) Kuchanov, S. I.; Pis'men, L. M. *Polym. Sci. USSR* **1971**, *13*, 2288.
- (4) Zhu, S. *J. Polym. Sci., Part B: Polym. Phys.* **1996**, *34*, 505.
- (5) Zhu, S.; Hamielec, A. E. *J. Polym. Sci., Part B: Polym. Phys.* **1994**, *32*, 929.
- (6) Tobita, H.; Zhu, S. *J. Polym. Sci., Part B: Polym. Phys.* **1996**, *34*, 2099.
- (7) Tobita, H. *Polym. React. Eng.* **1993**, *3*, 379.
- (8) Tobita, H. *J. Polym. Sci., Part B: Polym. Phys.* **1994**, *32*, 911.
- (9) Tobita, H. *J. Polym. Sci., Part B: Polym. Phys.* **1998**, *36*, 2015.
- (10) Dias, R. C. S.; Costa, M. R. P. F. N. *Macromolecules* **2003**, *36*, 8853.
- (11) Wulkow, M. *Macromol. Theory Simul.* **1996**, *5*, 393.
- (12) Iedema, P. D.; Hoefsloot, H. C. J. *Macromolecules* **2003**, *36*, 6632.
- (13) Tobita, H.; Hatanaka, K. *J. Polym. Sci., Part B: Polym. Phys.* **1995**, *33*, 841.

MA049275F